

This document is confidential and is proprietary to the American Chemical Society and its authors. Do not copy or disclose without written permission. If you have received this item in error, notify the sender and delete all copies.

Gas Phase Detection of Benzocyclopropenyl

Journal:	<i>The Journal of Physical Chemistry</i>
Manuscript ID	jp-2015-075094.R1
Manuscript Type:	Article
Date Submitted by the Author:	06-Oct-2015
Complete List of Authors:	Maity, Surajit; university of basel, chemistry Steglich, Mathias; university of basel, chemistry Maier, John; University of Basel, Department of Chemistry

SCHOLARONE™
Manuscripts

Gas Phase Detection of Benzocyclopropenyl

Surajit Maity,* Mathias Steglich, John P. Maier *

Department of Chemistry, University of Basel, Klingelbergstrasse 80, CH 4056, Basel,
Switzerland

Corresponding Author: surajit.maity@gmail.com, j.p.maier@unibas.ch

Abstract

The gas phase detection of benzocyclopropenyl is reported. In this aromatic resonance stabilized radical, a large angular strain is present due to a three membered ring annelated to a benzene. Resonant two-color two-photon ionization technique is used to record the $D_1(^2A_2) \leftarrow D_0(^2B_1)$ electronic transition of this radical after the in situ synthesis in a discharge source. The spectrum features absorptions up to 3300 cm^{-1} above the origin band at 19305 cm^{-1} . Benzocyclopropenyl is possibly the major product of the bimolecular reaction of benzene and an atomic carbon at low temperatures.

1. Introduction

The Laboratory investigations on the resonance stabilized radicals (RSRs) have been the subject of interest among the astrochemistry, combustion, atmospheric chemistry communities.¹⁻⁵ The RSRs play crucial roles in the formation of polycyclic aromatic hydrocarbons (PAHs) and soot particles in combustion systems. In the interstellar medium, the barrierless addition reactions of RSRs may lead to the formation of complex organic molecules including PAHs at low temperatures. Benzene has been considered as the first building block of PAH formation and detected in oxygen poor hydrocarbon flames.⁶ The discovery of benzene in the circumstellar medium,⁷ propelled the investigation of its reaction with small C/H species.^{8,9} The simplest of these reactions is the bimolecular reaction of benzene and atomic carbon which resulted in the synthesis of C₇H₅ isomers.⁸⁻¹⁵ Except for the most stable fulvenallenyl,¹⁶⁻¹⁹ literature data on the other isomers are sparse. Energetically the second most stable isomer is benzocyclopropenyl radical which depicts a benzene annelated to a three membered ring. Because of the large angular strain associated with the small ring, this class of molecular entities remains fascinating to the physical organic chemistry community.²⁰⁻²² They are suitable to verify the role of Mills-Nixon effect as well.²³ In this, two opposite phenomena, the delocalization energy of the π electrons (aromaticity) on the benzene moiety and the angular distortion due to the annelated small ring, are present. Both of these effects are exciting to organic chemistry community. The fused small rings are known to influence the reactivity and regioselectivity within the aromatic fragment.²⁴

Benzocyclopropenyl was mentioned as a reaction product in crossed molecular beam experiments in the reaction of benzene and atomic carbon.^{8,9,11,12,15} The reaction proceeds

1
2
3 through the formation of a cycloheptatetraene (C_7H_6) intermediate,^{13,14} followed by
4
5 atomic hydrogen elimination to produce C_7H_5 isomers. At collision energies of 8.8-52.5
6
7 kJ mol^{-1} , the major product was assigned as the dihydroheptatrienyl radical with an
8
9 estimated upper limit of 10% yield of the benzocyclopropenyl radical.⁹⁻¹¹ However, the
10
11 Rice–Ramsperger–Kassel–Marcus theory estimated ~90% for the yield at a low collision
12
13 energy of 1.3 kJ mol^{-1} .¹¹ In the interstellar medium and hydrocarbon rich planetary
14
15 atmospheres, the gas phase reaction is likely to occur at a low collision energy; therefore,
16
17 it is expected to be the major product. Here, the detection of benzocyclopropenyl is
18
19 reported in the gas phase. Its $D_1 \leftarrow D_0$ electronic transition is measured using a resonant
20
21 two-color two-photon ionization (R2C2PI) scheme coupled with a linear time-of-flight
22
23 mass spectrometer (TOF-MS).
24
25
26
27
28
29

30 2. Experimental

31
32 The experiments were conducted in a three-stage differentially pumped vacuum chamber
33
34 ($\sim 1.0 \times 10^{-7}$ mbar) operational with turbo pumps. A gas mixture of 0.1 % propyne and 0.1
35
36 % diacetylene in helium (backing pressure of 9.0 bar) was expanded by a pulsed valve
37
38 (~ 220 μs) into the source chamber to maintain 4.0×10^{-5} mbar. Simultaneously, a pulsed
39
40 (200 μs) high voltage electrical discharge (-600 V) was applied to produce the target
41
42 radical in a cold molecular beam. This was collimated by passing through a 2.0 mm
43
44 skimmer placed 50 mm downstream of the discharge source. It then entered the extraction
45
46 region of the TOF-MS positioned inside the second chamber. A potential of +300 V was
47
48 applied to the skimmer to repel the charged species produced along with the neutrals. A
49
50 counter-propagating signal output of an optical parametric oscillator laser (OPO, 5-10 ns;
51
52 20 Hz; 0.1 nm bandwidth, tuning range 410-710 nm, 2-8 mJ/pulse) excites the target
53
54
55
56
57
58
59
60

radicals to higher lying electronic states. The radicals are subsequently ionized by a fifth harmonic (212.8 nm) output of a Nd:YAG laser (1.5 mJ /pulse), introduced about 2-4 ns after the excitation laser. Only one Nd:YAG laser is used to pump the OPO and produce the 5th harmonic output (212.8 nm). This scheme eliminates temporal jitter between the pump and probe pulses. The resulting ions were extracted perpendicular to the molecular beam into the TOF tube connected with a two-stage acceleration setup and detected by a micro-channel plate. Higher-resolution scan of the origin band was carried out with a dye laser (≈ 10 ns; 10 Hz; 0.002 nm bandwidth) pumped by the third harmonic of a Nd:YAG laser. The dye laser output was calibrated with a wavelength meter. The pulsed valve, pulsed discharge voltage, extraction voltage and the laser pulses were synchronized by digital delay generators.

3. Results

The electronic spectrum of C₇H₅ radical (Figure 1) is recorded by monitoring the ion signal at $m/z = 89$ amu. The spectrum features multiple absorptions in the region 18600-22600 cm⁻¹, implying a strong Franck-Condon activity. The observed band positions and vibrational frequencies are summarized in Table 1. The strongest feature at 19305 cm⁻¹ (517.9 nm) assigned as the origin band of the D₁(²A₂)←D₀(²B₁) transition of the benzocyclopropenyl radical. Two weak features at 488 and 626 cm⁻¹ to the red are hot bands. The bands 528, 731, 921, 1124 and 1327 cm⁻¹ above the origin are separated by 196±7 cm⁻¹, implying combination of 528 cm⁻¹ and 203 cm⁻¹ vibrational frequencies. Furthermore, combinations of the low energy vibrations below 600 cm⁻¹ account for all the features up to 3300 cm⁻¹. These observations indicate a vibronic progression in the excited state. The high resolution recording of the origin band in Figure 2 exhibits three

1
2
3 peaks of unresolved *P*, *Q* and *R* branches. Electronic spectra are recorded at each *m/z*
4
5 between 12 and 250 amu, simultaneously. Other than a weak signal at the isotopic mass
6
7 of 90 ($^{13}\text{CC}_6\text{H}_5$), no other mass channels are identified with an electronic transition
8
9 similar to the reported spectrum. Therefore, any possibility of C_7H_5^+ (*m/z*=89 amu)
10
11 formation via a dissociation of higher mass product is ruled out.
12
13
14

15 16 **4. Discussion**

17
18
19 To identify the structure of the C_7H_5 carrier of the observed electronic band system with the
20
21 strongest band at 19305 cm^{-1} , density functional theory (DFT) and time-dependent DFT (TD-
22
23 DFT) calculations were carried out using the B3LYP functional and cc-pVDZ basis set with the
24
25 Gaussian-09 program package.²⁵ About 30 different C_7H_5 structures were optimized on both
26
27 singlet and triplet surfaces. The relative stability of the structures are in agreement with the
28
29 literature.^{10,18} The ground state geometries of the seven lowest energy C_7H_5 structures are shown
30
31 in Figure 3. The calculated relative energies, vertical ionization (IP) and excitation energies are
32
33 given in Table 2. The cyclic isomers C_7H_5 -A, B, C and D with C_{2v} symmetry are at least 20 kJ
34
35 mol^{-1} more stable than the C_s symmetry acyclic structures (C_7H_5 -E, F and G). The most stable
36
37 isomer is C_7H_5 -A (fulvenallenyl radical).
38
39
40
41
42

43
44 At 19305 cm^{-1} , the experimental ionization limit of the two-photon process (8.22 eV) is close
45
46 to the IP of C_7H_5 -A, determined experimentally (8.19 eV)¹⁹ and computationally (8.1 eV, Table
47
48 2). However, this structure is excluded as the carrier of the band system because of two reasons.
49
50 Firstly, the ion signal at *m/z* = 89 can be detected at two-photon energies as low as 7.6 eV
51
52 (Supporting Information Figure S1). Secondly, the vertical excitation energies of the symmetry
53
54 allowed $\text{D}_1(^2\text{A}_2)\leftarrow\text{D}_0(^2\text{B}_1)$ and $\text{D}_3(^2\text{B}_1)\leftarrow\text{D}_0(^2\text{B}_1)$ transitions are 0.93 and 3.26 eV, which
55
56
57
58
59
60

1
2
3 disagree with the experimental value of 2.39 eV. The $D_2(^2B_2) \leftarrow D_0(^2B_1)$ energy (2.73 eV) is
4
5 close, but is a symmetry forbidden transition. Based on this, fulvenallenyl radical C_7H_5-A is
6
7 expected to have an electronic transition in the UV region and is unlikely to have a contribution
8
9 in the present spectrum. All other isomers have predicted vertical IPs in the 6.0-7.4 eV range and
10
11 are detectable within the experimental limits. In the case of C_7H_5-C , the calculated vertical
12
13 transition energy for $D_2(^2A_2) \leftarrow D_0(^2B_1)$ is close (2.54 eV) to the experimental value (2.39 eV),
14
15 however, the oscillator strength is zero. No other transitions for the isomer C_7H_5-C and none for
16
17 C_7H_5-D agree with the observed band energy. Therefore, both structures C_7H_5-C and D are ruled
18
19 out as possible carriers.
20
21
22
23

24 The remaining isomers C_7H_5-B , E, F and G are characterized by at least one transition close
25
26 (0.02-0.33 eV) to the experimental value. The isomer C_7H_5-B is the second lowest structure
27
28 (Table 2) on the doublet potential energy surface and is at least 59 kJ mol^{-1} more stable than the
29
30 other. The $D_1(^2A_2) \leftarrow D_0(^2B_1)$ excitation energy of isomer C_7H_5-B is the closest (2.41) to the
31
32 experimental value of 2.39 eV compared to the allowed $D_2(^2A'') \leftarrow D_0(^2A'')$ electronic transition
33
34 of C_7H_5-E , F and G. Therefore, isomer C_7H_5-B is the likely carrier of the observed band system.
35
36 To verify this, the high resolution scan of the 19305 cm^{-1} band is compared with the rotational
37
38 profiles, simulated using PGOPHER,²⁷ for the electronic transitions $D_1(^2A_2) \leftarrow D_0(^2B_1)$ of C_7H_5-B
39
40 and $D_2(^2A'') \leftarrow D_0(^2A'')$ of C_7H_5-E , F and G. As shown in Figure 2 and SI Figure S2, the best
41
42 agreement is achieved with isomer C_7H_5-B . The simulated *b*-type rotational profile obtained at
43
44 $T \sim 7 \text{ K}$ for C_7H_5-B provides a good agreement with the high resolution recording. The best fit
45
46 parameters $A''=0.180$, $B''=0.107$, $C''=0.075$, $A'=0.179$, $B'=0.110$ and $C'=0.074$ are within $\pm 5 \%$
47
48 of the calculated values in the D_0 electronic state, $A''=0.187$, $B''=0.115$, $C''=0.071$. The above
49
50
51
52
53
54
55
56
57
58
59
60

1
2
3 supports the assignment of benzocyclopropenyl radical (C_7H_5-B) with the $D_1(^2A_2) \leftarrow D_0(^2B_1)$
4 origin band at 19305 cm^{-1} .
5
6

7
8 To assign the experimental frequencies of C_7H_5-B excited in the D_1 state, the calculation of
9 the normal modes in this state was attempted. However, repeated efforts to locate the fully
10 relaxed geometry in the D_1 state were unsuccessful. Therefore, a prediction of the intensity
11 pattern for the $D_1(^2A_2) \leftarrow D_0(^2B_1)$ band system using Franck-Condon-Herzberg-Teller method
12 would be unreliable. A first order saddle point is found with a C_{2v} geometry similar to the ground
13 state structure. The prominent hot band observed 488 cm^{-1} below the origin band agrees with the
14 ground state vibrational frequency calculated at 488 cm^{-1} (ν_{30}). The observed low energy
15 vibrational frequencies $203, 434, 454$ and 481 cm^{-1} above the origin band can be linked to
16 bending modes belonging to a_2 and b_2 symmetries (Supporting Information). An unambiguous
17 assignment of the vibrational frequencies is hard to achieve based on the ground state normal
18 modes. The observation of the asymmetric modes via vibronic mixing clearly implies a bent
19 excited D_1 state. The C_{2v} symmetric saddle point in the D_1 state also supports this.
20
21
22
23
24
25
26
27
28
29
30
31
32
33
34
35

36 It is worth to mention that the rotational contours for the $D_2(^2A'') \leftarrow D_0(^2A'')$ electronic
37 transitions of C_s symmetry isomers C_7H_5-E, F and G (Figure 2, SI Figure S2) show prominent K -
38 stacks in both b - and a -type electronic transitions. The vibrational patterns calculated via a
39 Franck-Condon-Herzberg-Teller approach (FCHT)²⁶ for that transition of the above isomers
40 show poor agreement with the experimental spectrum (SI Figure 3). This reinforces the
41 assignment to benzocyclopropenyl radical.
42
43
44
45
46
47
48
49
50

51 **5. Summary**

52
53
54 The gas phase electronic spectrum of a C_7H_5 radical, benzocyclopropenyl radical, is
55 measured for the first time using R2C2PI scheme. The radical is synthesized via an electrical
56
57
58
59
60

1
2
3 discharge of a hydrocarbon gas mixture. The $D_1(^2A_2) \leftarrow D_0(^2B_1)$ electronic transition is observed
4
5 in the 18600-22600 cm^{-1} region with the origin band at 19305 cm^{-1} . The high resolution
6
7 recording of the 19305 cm^{-1} band assists the spectral assignment. Vibronic features up to 3300
8
9 cm^{-1} originate from combinations of the low energy modes. The spectral data can be used to
10
11 verify the formation of benzocyclopropenyl in the reaction of benzene and atomic carbon and
12
13 understand its role in both combustion and astrophysical environments.
14
15

16
17
18 **Supporting Information Available.** Ground state calculated harmonic frequencies of C_7H_5-B ,
19
20 ionization efficiency curve, simulated rotational profiles and FCHT simulations of $D_1 \leftarrow D_0$ (for
21
22 C_7H_5-B) and $D_2 \leftarrow D_0$ electronic transitions for C_7H_5 isomers are given. This material is available
23
24 free of charge via the Internet at <http://pubs.acs.org>.
25
26
27

28 29 **Acknowledgment**

30
31 This work is funded by the Swiss National Science Foundation (Project 200020-140316/1)
32
33

34 35 **References**

- 36
37 (1) McEnally, C. S.; Pfefferle, L. D.; Atakan, B.; Kohse-Höinghaus, K. Studies of Aromatic
38
39 Hydrocarbon Formation Mechanisms in Flames: Progress Towards Closing the Fuel Gap.
40
41 *Prog. Energy Combust. Sci.* **2006**, *32*, 247-294.
42
43 (2) Miller, J. A.; Melius, C. F. Kinetic and Thermodynamic Issues in the Formation of
44
45 Aromatic Compounds in Flames of Aliphatic Fuels. *Combust. Flame* **1992**, *91*, 21-39.
46
47 (3) Gobbi, A.; Frenking, G. Resonance Stabilization in Allyl Cation, Radical, and Anion. *J.*
48
49 *Am. Chem. Soc.* **1994**, *116*, 9275-9286.
50
51 (4) McMillen, D. F.; Trevor, P. L.; Golden, D. M. Highly Stabilized Radicals: Benzylic
52
53 Radicals in Polycyclic Aromatic Systems. *J. Am. Chem. Soc.* **1980**, *102*, 7400-7402.
54
55
56
57
58
59
60

- 1
2
3
4 (5) Wong, M. W.; Pross, A.; Radom, L. Addition of Tert-Butyl Radical to Substituted
5 Alkenes: a Theoretical-Study of the Reaction-Mechanism. *J. Am. Chem. Soc.* **1994**, *116*,
6 11938-11943.
7
8
9 (6) Marinov, N. M.; Pitz, W. J.; Westbrook, C. K.; Castaldi, M. J.; Senkan, S. M. Modeling
10 of Aromatic and Polycyclic Aromatic Hydrocarbon Formation in Premixed Methane and
11 Ethane Flames. *Combust. Sci. Tech.* **1996**, *116*, 211-287.
12
13
14 (7) José, C.; Ana, M. H.; Tielens, A. G. G. M.; Juan, R. P.; Fabrice, H.; Michel, G.; Waters,
15 L. B. F. M. Infrared Space Observatory's Discovery of C₄H₂, C₆H₂, and Benzene in CrI 618.
16 *Astrophys. J. Lett.* **2001**, *546*, L123-L126.
17
18
19 (8) Kaiser, R. I.; Asvany, O.; Lee, Y. T. Crossed Beam Investigation of Elementary
20 Reactions Relevant to the Formation of Polycyclic Aromatic Hydrocarbon (PAH)-Like
21 Molecules in Extraterrestrial Environments. *Planet. Space Sci.* **2000**, *48*, 483-492.
22
23
24 (9) Kaiser, R. I.; Vereecken, L.; Peeters, J.; Bettinger, H. F.; Schleyer, P. v. R.; Schaefer, H.
25 F. Elementary Reactions of the Phenyl Radical, C₆H₅, with C₃H₄ Isomers, and of Benzene,
26 C₆H₆, with Atomic Carbon in Extraterrestrial Environments. *Astron. Astrophys.* **2003**, *406*,
27 385-391.
28
29
30 (10) da Silva, G. Reaction of Benzene with Atomic Carbon: Pathways to Fulvenallene and
31 the Fulvenallenyl Radical in Extraterrestrial Atmospheres and the Interstellar Medium. *J.*
32 *Phys. Chem. A* **2014**, *118*, 3967-3972.
33
34
35 (11) Hahndorf, I.; Lee, Y. T.; Kaiser, R. I.; Vereecken, L.; Peeters, J.; Bettinger, H. F.;
36 Schreiner, P. R.; Schleyer, P. v. R.; Allen, W. D.; Schaefer, H. F. A Combined Crossed-
37 Beam, Ab Initio, and Rice-Ramsperger-Kassel-Marcus Investigation of the Reaction of
38 Carbon Atoms C(³P_j) with Benzene, C₆H₆(X ¹A_{1g}) and D₆-Benzene, C₆D₆(X ¹A_{1g}). *J. Chem.*
39 *Phys.* **2002**, *116*, 3248-3262.
40
41
42 (12) Bettinger, H. F.; Schleyer, P. v. R.; Schaefer, H. F.; Schreiner, P. R.; Kaiser, R. I.; Lee,
43 Y. T. The Reaction of Benzene with a Ground State Carbon Atom, C(³P_j). *J. Chem. Phys.*
44 **2000**, *113*, 4250-4264.
45
46
47 (13) McKee, M. L.; Reisenauer, H. P.; Schreiner, P. R. Combined Ab Initio Molecular
48 Dynamics and Experimental Studies of Carbon Atom Addition to Benzene. *J. Phys. Chem.*
49 *A* **2014**, *118*, 2801-2809.
50
51
52
53
54
55
56
57
58
59
60

- 1
2
3
4 (14) Krasnokutski, S. A.; Huisken, F. Ultra-Low-Temperature Reactions of C(³P_j) Atoms
5 with Benzene Molecules in Helium Droplets. *J. Chem. Phys.* **2014**, *141*, 214306.
6
7
8 (15) Kaiser, R. I.; Hahndorf, I.; Huang, L. C. L.; Lee, Y. T.; Bettinger, H. F.; Schleyer, P. V.
9 R.; Schaefer, H. F.; Schreiner, P. R. Crossed Beams Reaction of Atomic Carbon, C(³P_j),
10 with D₆-Benzene, C₆D₆ (X¹A_{1g}): Observation of the per-Deutero-1,2-Didehydro-
11 Cycloheptatrienyl Radical, C₇D₅ (X²B₂). *J. Chem. Phys.* **1999**, *110*, 6091-6094.
12
13
14 (16) da Silva, G.; Trevitt, A. J. Chemically Activated Reactions on the C₇H₅ Energy
15 Surface: Propargyl + Diacetylene, i-C₅H₃+Acetylene, and n-C₅H₃+Acetylene. *Phys. Chem.*
16 *Chem. Phys.* **2011**, *13*, 8940-8952.
17
18
19
20 (17) Botschwina, P.; Oswald, R. Fulvenallenyl Cation (C₇H₅⁺) and Its Complex with an
21 Argon Atom: Results of High-Level Quantum-Chemical Calculations. *J. Phys. Chem. A*
22 **2012**, *116*, 3448-3453.
23
24
25
26 (18) da Silva, G.; Trevitt, A. J.; Steinbauer, M.; Hemberger, P. Pyrolysis of Fulvenallene
27 (C₇H₆) and Fulvenallenyl (C₇H₅): Theoretical Kinetics and Experimental Product Detection.
28 *Chem. Phys. Lett.* **2011**, *517*, 144-148.
29
30
31
32 (19) Steinbauer, M.; Hemberger, P.; Fischer, I.; Bodi, A. Photoionization of C₇H₆ and C₇H₅:
33 Observation of the Fulvenallenyl Radical. *ChemPhysChem* **2011**, *12*, 1795-1797.
34
35
36 (20) Apeloig, Y.; Arad, D. Cyclopropabenzene. Geometry, Electronic Structure, Strain,
37 Reactivity, and the Question of Bond Fixation. A Theoretical Study. *J. Am. Chem. Soc.*
38 **1986**, *108*, 3241-3247.
39
40
41
42 (21) Eckert-Maksić, M.; Maksić, Z. B.; Hodošček, M.; Poljanec, K. Mills-Nixon Effect in
43 Heteroanalogs of Cyclopropabenzene. *Int. J. Quantum Chem.* **1992**, *42*, 869-877.
44
45
46 (22) Maksic, Z. B.; Eckert-Maksić, M.; Pfeifer, K.-H. Reversed Mills-Nixon Effect in
47 Benzoborirene and Benzocyclopropenyl Cations. *J. Mol. Struct.* **1993**, *300*, 445-453.
48
49
50 (23) Mills, W. H.; Nixon, I. G. Stereochemical Influences on Aromatic Substitution.
51 Substitution Derivatives of 5-Hydroxyhydrindene. *J. Chem. Soc.* **1930**, 2510-2524.
52
53
54
55
56
57
58
59
60

1
2
3
4 (24) Eckert-Maksić, M.; Glasovac, Z.; Novak Coumbassa, N.; Maksić, Z. B. The Mills-
5 Nixon Effect and Chemical Reactivity-Methyl Cation Affinity of Some Cycloalkabenzenes.
6 *J. Chem. Soc., Perkin Trans. 2* **2001**, 1091-1098.
7

8
9 (25) Frisch, M. J.; Trucks, G. W.; Schlegel, H. B.; Scuseria, G. E.; Robb, M. A.;
10 Cheeseman, J. R.; Scalmani, G.; Barone, V.; Mennucci, B.; Petersson, G. A.; al., e. Gaussian
11 09; Gaussian, Inc.: Wallingford, CT, USA, 2009.
12

13
14 (26) Barone, V.; Bloino, J.; Biczysko, M. Vibrationally-Resolved Electronic Spectra in
15 Gaussian 09, 2009.
16
17

18
19 (27) Western, C. M. Pgopher, a Program for Simulating Rotational Structure, University of
20 Bristol, [Http://Pgopher.Chm.Bris.Ac.Uk](http://Pgopher.Chm.Bris.Ac.Uk), 2014.
21
22
23
24
25
26
27
28
29
30
31
32
33
34
35
36
37
38
39
40
41
42
43
44
45
46
47
48
49
50
51
52
53
54
55
56
57
58
59
60

TOC Graphic

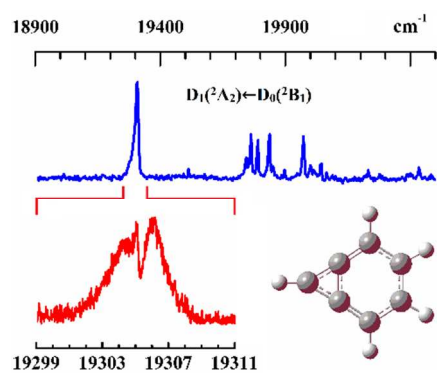


Table 1. Absorption bands and vibrational frequencies relative to the origin band in the $D_1(^2A_2) \leftarrow D_0(^2B_1)$ electronic transition of benzocyclopropenyl radical.

nm	cm^{-1}	$\Delta\nu$ (cm^{-1})	Tentative Assignment
535.2	18679	-626	
531.3	18817	-488	30_1^0
517.9	19305	0	0_0^0
512.5	19508	203	20_0^1
506.5	19739	434	18_0^1
506.0	19759	454	15_0^1
505.3	19786	481	
504.1	19833	528	30_1^1
503.7	19849	544	11_0^1
502.6	19892	587	
501.2	19948	643	
500.7	19968	663	
500.0	19996	691	
499.6	20012	707	
499.0	20036	731	
494.3	20226	921	
489.4	20429	1124	
484.5	20632	1327	
482.9	20704	1399	
478.4	20899	1594	
476.9	20964	1659	
474.0	21089	1784	
465.8	21464	2159	
452.5	22091	2786	
442.5	22590	3285	

Table 2. The zero-point energy corrected relative stability (E) in kJ mol^{-1} , vertical ionization energy (IP) and excitation energies (ΔE) of $D_{1-3} \leftarrow D_0$ transitions of C_7H_5 isomers in eV. The oscillator strength (f) of each transition is given.

Isomer	E	IP	ΔE		f
			D ₁₋₃	eV (nm)	
C ₇ H ₅ -A	0	8.1	D ₁ (² A ₂)	0.93 (1335)	0.000
			D ₂ (² B ₂)	2.73 (453)	0.000
			D ₃ (² B ₁)	3.26 (380)	0.006
C ₇ H ₅ -B	45	6.4	D ₁ (² A ₂)	2.41(514)	0.004
			D ₂ (² A ₂)	3.53(351)	0.018
			D ₃ (² B ₁)	3.74(331)	0.021
C ₇ H ₅ -C	74	6.8	D ₁ (² A ₂)	1.46 (847)	0.001
			D ₂ (² A ₂)	2.54 (488)	0.000
			D ₃ (² B ₁)	3.91 (317)	0.001
C ₇ H ₅ -D	86	6.0	D ₁ (² A ₂)	1.10 (1124)	0.001
			D ₂ (² B ₂)	1.72 (719)	0.000
			D ₃ (² A ₁)	3.87 (321)	0.001
C ₇ H ₅ -E	104	7.3	D ₁ (² A')	2.18 (569)	0.000
			D ₂ (² A'')	2.50 (495)	0.005
			D ₃ (² A')	3.19 (388)	0.000
C ₇ H ₅ -F	105	7.3	D ₁ (² A')	2.55 (486)	0.000
			D ₂ (² A'')	2.72 (455)	0.030
			D ₃ (² A')	3.28 (378)	0.000
C ₇ H ₅ -G	111	7.4	D ₁ (² A')	2.58 (481)	0.000
			D ₂ (² A'')	2.65 (468)	0.019
			D ₃ (² A')	3.30 (375)	0.000

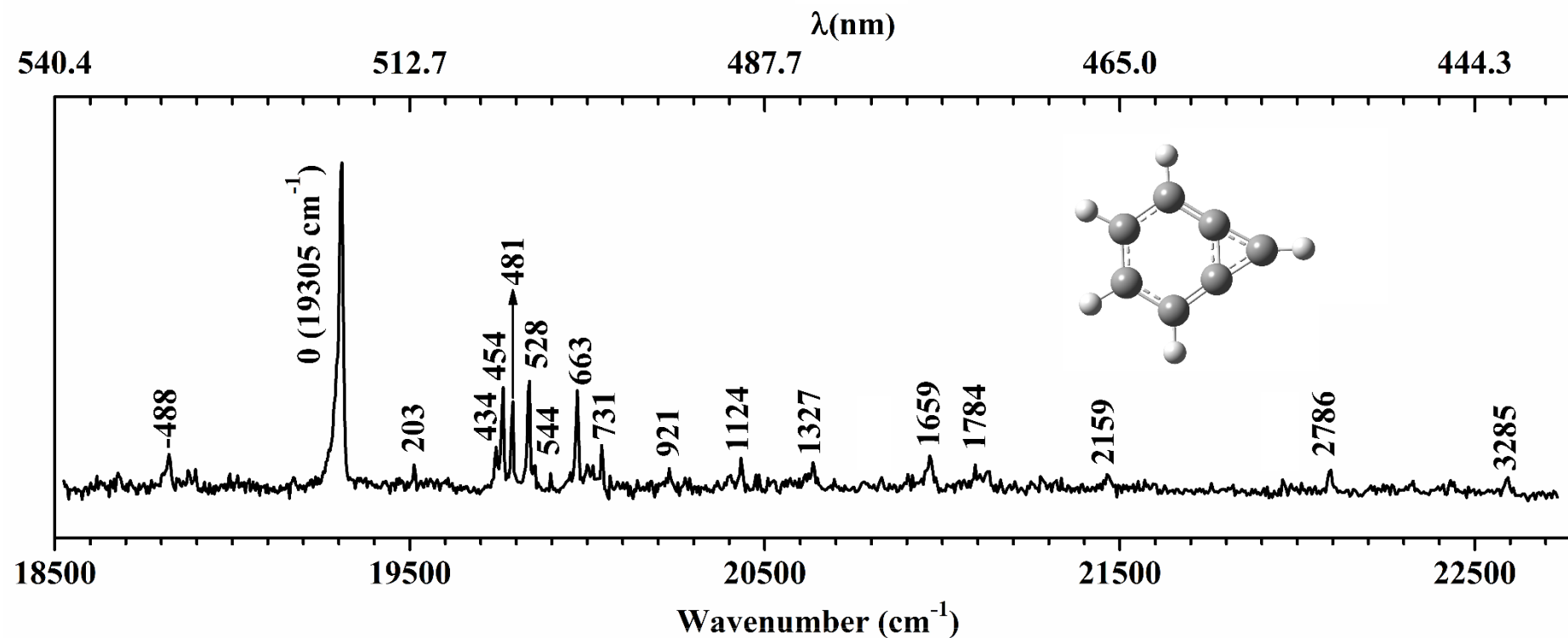


Figure 1. Resonant two-color two-photon ionization spectrum of benzocyclopropenyl radical (C_7H_5).

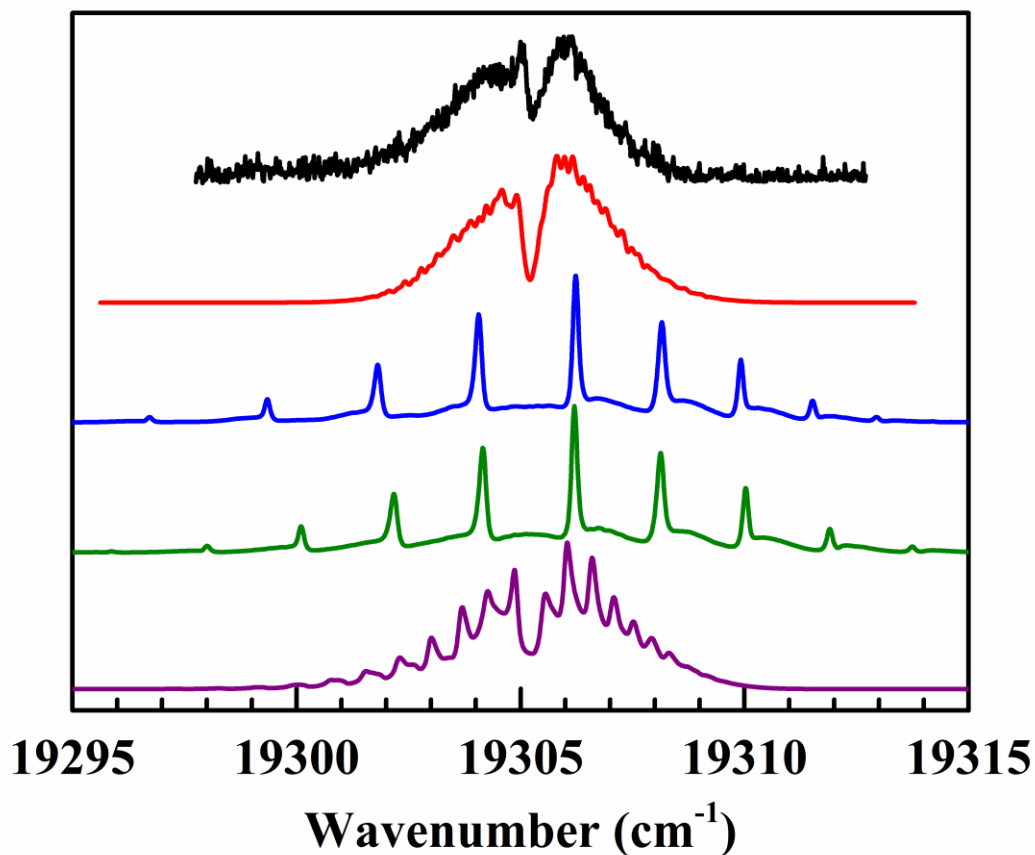


Figure 2. The origin band in the $D_1(^2A_2) \leftarrow D_0(^2B_1)$ electronic spectrum of benzocyclopropenyl radical measured at a resolution of 0.08 cm^{-1} (black trace) and the simulated *b*-type rotational contour at $T=7 \text{ K}$ (red). The *b*-type rotational contours ($D_2(^2A'') \leftarrow D_0(^2A'')$) obtained for the C_s symmetry isomers $C_7H_5\text{-E}$ (blue), $C_7H_5\text{-F}$ (green), $C_7H_5\text{-G}$ (purple) are shown for comparison. Contour simulations obtained for the *a*-type transitions are given in the Supporting Information.

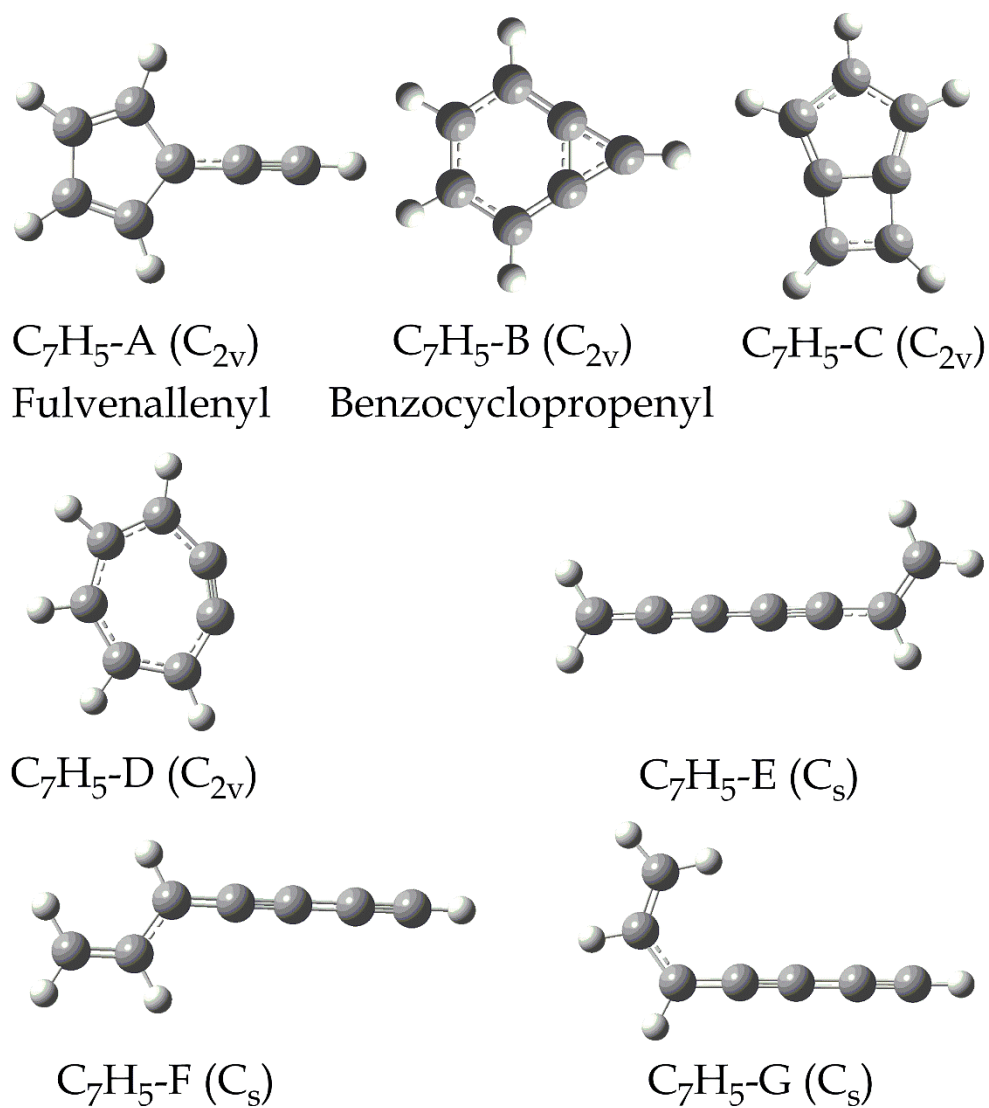


Figure 3. The ground state geometries of C_7H_5 isomers.